Detection of morphotropic phase boundary in A-site/Ca-substituted Na0.5Bi0.5TiO3 complex oxides ferroelectric system

Roy Roukos, Sara Abou Dargham, Jimmy Romanos, Denis Chaumont

Detection of Morphotropic Phase Boundary in A-site/Ca–substituted $Na_{0.5}Bi_{0.5}TiO_3$ Complex Oxides Ferroelectric System

Roy Roukos[a,*], Sara Abou Dargham[b], Jimmy Romanos[b], Denis Chaumont[a]

[a] *Laboratoire Interdisciplinaire Carnot de Bourgogne UMR 6303 CNRS, Université de Bourgogne, 9 Avenue Alain Savary, 21078 Dijon, France*
[b] *Department of Natural Sciences, Lebanese American University, P.O. Box 36, Byblos, Lebanon*

Abstract

Vibrational and structural properties of lead-free piezoelectric (1-x)$Na_{0.5}Bi_{0.5}TiO_3$–x$CaTiO_3$ ($0 \leq x \leq 1.00$) solid solutions have been investigated using Raman spectroscopy and X-ray diffraction. Different anomalies were detected and analyzed taking into consideration the phase transition from rhombohedral to orthorhombic phase at room temperature. All Raman bands were interpreted through the variation in the peak positions (frequency) and the corresponding half-widths at half maximum (HWHM) as a function of x. XRD used as a complementary technique to Raman spectroscopy, showed that the rhombohedral – orthorhombic phase transition went gradually through an intermediate phase consisting of a mixture of rhombohedral *(R3c)* and orthorhombic *(Pnma)* structures and that the fraction of orthorhombic phase increased with CT composition. The results show that the morphotropic phase boundary (MPB) is located between 0.09 and 0.15.

Keywords: Morphotropic phase boundary (MPB), Raman spectroscopy, X-ray diffraction, NBT-CT, Ferroelectric

1. Introduction

In the last few decades, the structure and phase instabilities were widely studied in solid solutions ferroelectric materials. In particular, these instabilities are mostly responsible for enhancing the dielectric and piezoelectric properties of ferroelectric lead-oxides ceramic materials [1, 2]. $PbZr_{(1-x)}Ti_xO3$, known as PZT, are the most investigated complex-structured solid solutions. These materials are used in the electronics industry for different applications such as electrostrictive, sensors, transducers, etc. The most interesting solid solution of PZT lies around x = 0.50 corresponding to the limit separating the rhombohedral and tetragonal ferroelectric phases [3], which is called "Morphotropic Phase Boundary" (MPB). The term

*Corresponding author.
Email address: roy.roukos@gmail.com (Roy Roukos)

"MPB" is currently used to refer to an imaginary border related to the phase transitions due to changes in compositions at room temperature [4]. Similarly to PZT, the interest has widely arisen since the MPB was recently reported to separate the two phases in lead-free systems which is accompanied by a significant improvement in the dielectric permittivity, electromechanical and piezoelectric properties [5, 6]. Taking into consideration the impact of Pb on the environment, several research groups have investigated Pb-free systems exhibiting MPB. $Na_{0.5}Bi_{0.5}TiO_3$ (NBT) is considered as one of the potential candidates to replace Pb-based piezoceramics, due to its ability to form complex perovskite solid solutions with other ferroelectric perovskites, such as BaTiO3 (BT) [2, 7–9], $(K_{0.5}Bi_{0.5})TiO_3$ (KBT) [10–12] and $SrTiO_3$ (ST) [13–15] where interesting piezoelectric properties are shown close to their MPB. The presence of different atoms at A-site relaxor perovskite shows a particular phase transition sequence, making these systems more attractive [16–18].

Despite numerous studies made on A-site cation-substituted, the exact locations of MPB in most solid solutions are still inconclusive. For example, the (1-x)NBT – ST system has been shown great interest since the discovery of MPB. This system forms solid solutions with MPB located towards x = 0.20, between the rhombohedral phase *(R3c)* and the cubic/pseudocubic phase *(Pm3m)* [14]. Different authors have studied this system to determine the composition range of the MPB and to establish its physical and structural properties. Despite the various techniques used, it is shown that the existence of an MPB depends on the studies, leading to different ranges of MPB [14, 19–22]. However, some research did not obtain the MPB composition regardless of the percentage of doping (x) and proved that its existence is still not clear; therefore the system only exhibited a relaxor behavior [15].

Park et al. [19] suggested that the rhombohedral phase of NBT transits diffusely into a cubic phase with increasing ST ($x > 0.26$), similarly to the diffuse phase transition obtained in relaxor ferroelectrics as a function of temperature. In contrast, Gomah-Pettry et al. [20] reported a first-order phase transition to a cubic phase for $x \geq 0.30$, where lately proved the existence of MPB separating two phases around $x \approx 0.25$ [13]. On the other hand, Hiruma et al. [22] attributed the existence of MPB around the composition range between 0.26 and 0.28 to the large electrostrain response (S = 0.29%) and to the enhancement of piezoelectric properties (normalized-strain d^*_{33} = 488 pm/V). Recently, Rout et al. [14] obtained distinct and discontinuous changes in dielectric properties at $x \approx 0.20$, revealing the presence of MPB. For this reason, the (1-x)NBT–xST is comparable to the (1-x)NBT–xCT system chosen in this study. It is important to note that the inconsistency in determination the exact location of MPB compositions are possibly related to different synthesis methods (conventional solid solution, hydrothermal, sol-gel), usage of single crystal or polycrystalline, as well as the process parameters (calcination and sintering time and temperature, cooling process, and using some additives during the samples preparation).

It has become relevant to investigate the development of the orthorhombic phase *(Pnma)* in solid solutions with CT, since the discovery of the *Pnma* phase in pure NBT [18, 23]. CT is considered as a typical paraelectric perovskite with *Pnma* orthorhombic symmetry at room temperature. It is possible to form solid solutions with CT-substituted NBT at A-site where an MPB composition is identified via a phase transition separating rhombohedral and orthorhombic phase due to changes in composition at room temperature. Recently,

such studies carried out by neutron diffraction on (1-x)NBT –xCT [24, 25], focusing on the superstructure and the calculation of phase tilt angle of the oxygen octahedra, revealed that the system exhibits two coexistent rhombohedral and orthorhombic *(R3c + Pnma)* phases for x = 0.15. The system is rhombohedral *(R3c)* for x $\leq$ 0.05 and orthorhombic *(Pnma)* for x $\geq$ 0.15. Moreover, Du et al. [26] identified the MPB around 0.08 $\leq$ x $<$ 0.14 where the rhombohedral and orthorhombic symmetries coexist. In a recent work [27], we reported a thermal hysteresis by dielectric properties of (1-x)NBT– xCT in a specific range of composition (x) and attributed that to the mixture and the interaction of two phases *(R3c + Pnma)*. In addition, Birks et al. [28] described the sample x = 0.10 by a pure orthorhombic symmetry *(Pnma)* at room temperature without detecting an MPB compositions which is very clear by the relaxor behavior obtained by dielectric properties. In the other hand, we reported that for x = 0.10 a complex structural behavior resulting a thermal hysteresis due to the interaction between the mixture of two phases rhombohedral *(R3c)* + orthorhombic *(Pnma)* [27]. Furthermore, we identified and quantified a relaxor behavior for this system, even for low concentration of CT (0 $\leq$ x $\leq$ 0.07) [29].

Raman spectroscopy is considered a sensitive technique for studying structural phase transition in perovskite-based solid solution systems exhibiting MPB. Raman spectra of NBT [30, 31] and various NBT-based solid solutions [14, 32, 33] are commonly available in the literature. However, a detailed comprehensive Raman investigation for (1-x)NBT– xCT system has not been reported yet. Consequently, a Raman scattering study of this system as a function of composition at room temperature would give a valuable contribution to understand the structural phase transition for the new compound NBT– CT. In this work, a detailed Raman scattering and X-ray diffraction (XRD) studies of (1-x)NBT–xCT (0 $\leq$ x $\leq$ 1.00) system were conducted at room temperature to detect the structural phase transition and specifically to determine the location and highlight the limit (border) of MPB composition with increasing CT concentration. To our knowledge, this is the first attempted to fit Raman spectra, and the obtained results were combined with XRD results to highlight the composition-dependent phase transitions at room temperature.

2. Experimental

Solid-state reaction method was used to prepare powder and ceramic samples in the form of solid solutions with various fractions of NBT and CT. The complex perovskite oxides with the general formula (1-x)NBT– xCT contains different values of compositional concentration between 0.00 and 1.00 (x = 0.00, 0.01, 0.05, 0.07, 0.09, 0.10, 0.11, 0.13, 0.15, 0.20, 0.22, 0.25, 0.27, 0.30, 0.35, 0.45, 0.55, 0.65, 0.75, 0.85, 0.95 and 1.00). This procedure consists of mixing stoichiometric amounts of high purity ($>$ 99.6%) reagent-grade powders of Bi_2O_3 (Alfa Aesar), TiO_2 (Alfa Aesar), Na_2CO_3(Prolabo) and $CaCO_3$ (Alfa Aesar). The mixtures were milled and homogenized inside a turbula using zirconia balls in water for 2 hours and then dried at 100 °C. Mixed powders were firstly calcined at 750 °C for 4 hours followed by another calcination at 950 °C for 4 hours in order to complete the chemical reaction of the formation of the desired compounds. The obtained powders were uniaxially pressed into disks of 13 mm diameter. Finally, the pellets were sintered at various temper-

atures between 1075 °C and 1350 °C for 1 hour in a confined environment. The optimum sintering temperature for producing highly dense ceramics was determined as a function of CT concentration. The obtained densities were in the range of 96 – 99%.

The phase identification and the crystallinity of both powders and ceramics were investigated by X-ray diffraction (XRD) using a D8 advance X-ray diffractometer (Vantec detector) with CuKα radiations λ = 1.5405 Å. XRD patterns were recorded at room temperature in the 2θ range from 20° to 90° with a step size of 0.017° and a counting time of 10 s/step. Raman spectra of (1-x)NBT–xCT system were registered between frequency range 4.00 and 700 cm^{-1} at room temperature using Jobin-Yvon T64000 spectrometer HR (high resolution). This system is equipped with Ar^{+} laser at 514.5 nm and 20 mW for excitation. The obtained results were analyzed by fitting the spectra to the Lorentzian and Gaussian line shape using the Fityk software to determine the band positions for each substitution rate.

3. Results

3.1. Raman spectroscopy and phonon behavior at room temperature

3.1.1. NBT and CT solid solutions reference spectra

NBT is a classical example of ferroelectric material with rhombohedral *(R3c)* symmetry at room temperature with 13 Raman-active modes. Its irreducible representation is: $\Gamma_{R3c} = 4A_1 + 9E + 4A_2$ where the A_2 mode is inactive in Raman. Figure 1(a) shows the Raman spectrum with its deconvolution into Lorentzian and Gaussian functions. The deconvolution of the total NBT spectrum shows 5 characteristics bands centered at 25 (A), 138 (B), 286 (C), and 530-584 (D) cm^{-1}. It is important to note that the obtained modes are less than expected due to the degenerescence of some phonon frequencies and/or to the insufficient intensities emitted from small polarizability of some modes. The obtained NBT spectrum is identical to that reported previously [32, 34, 35]. The overall spectral bands are relatively broad due to the polycristalline nature of the material and the disorder at A-site (simultaneous presence of Na^{+}/Bi^{3+} ions) which leads to the overlapping of some Ramgaian bands. The first band (A) is associated with Bi–O vibration (A_1 symmetry) and the second band (B) with Na–O vibration (A_1 symmetry). While the Na/Bi ions are occupying the A-site, the difference in the A-band location is due to the large difference in the masses of Na and Bi ions. The band (C) is attributed to the vibration of Ti–O bond, whereas the two overlapping bands (D) are dominated by vibrations of the oxygen atom and more precisely to vibrations of TiO_6 octahedra.

On the other hand, the CT is a typical paraelectric perovskite with orthorhombic *(Pnma)* phase at room temperature. It yields 24 Raman-active phonon modes as follow: $7Ag+5B_{1g}+7B_{2g}+5B_{3g}$. Room temperature Raman spectrum of CT is shown in figure 1(b). The obtained CT spectrum is in agreement with previous reports [36, 37]. The band at 641 $cm^{-1}$is attributed to the stretching vibration of Ti–O bond. Those centered at 470 and 494 $cm^{-1}$are assigned to the vibration of TiO_6 octahedra, while the bands between 227 - 340 $cm^{-1}$are attributed to the rotation of oxygen octahedra. Moreover, the two low frequencies

mode centered at 153 cm^{-1} and 183 cm^{-1} are due to vibration and motion of A-site ions i.e. Ca–O.

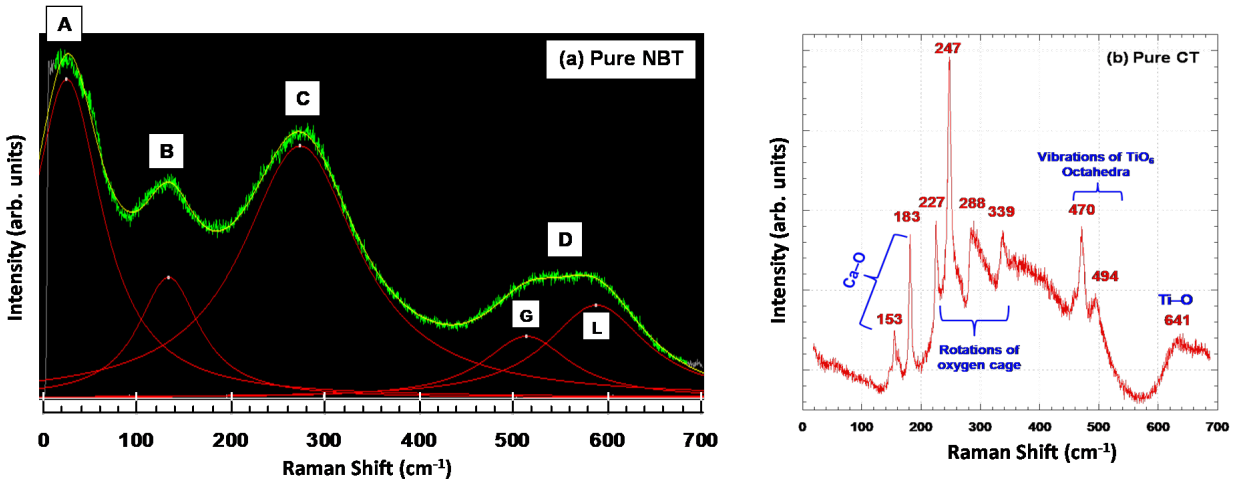

Figure 1: (a) Room temperature deconvoluted Raman spectrum of pure NBT solid solution according to five modes (Lorentzian and Gaussian) and (b) Raman spectrum of pure CT at room temperature.

3.1.2. (1-x)NBT–xCT solid solutions

Based on the irreducible representation of optical phonons for NBT and CT solid solutions, it is expected that additional modes will appear and disappear with increasing CT concentration due to the high number of Raman-active modes of CT compared to NBT. Furthermore, the substitution by long-range chemical order in orthorhombic paraelectric phase does not split any mode; instead, it deteriorates certain modes similar to TiO_6 octahedra (overlapping bands). Although the two materials are different, the vibration modes appear in the same frequency range (same type of vibration). For instance, at low frequency (NBT: 25 – 138 cm^{-1} and CT: 153 – 183 cm^{-1}), the A-site ions vibration is detected in both materials. Similarly, at high frequency (NBT: 530 – 584 $cm^{-1}$and CT: 470 – 494 cm^{-1}) the vibration of B-site is related to Ti–O and TiO_6 octahedra.

As the Raman spectra of NBT and CT are substantially different, it is possible to study their evolution as a function of x composition for (1-x)NBT–xCT solid solutions / $0.01 \leq x \leq 0.95$. The evolution of these spectra at room temperature is shown in figure 2. The qualitative analysis of figure 2 reveals significant changes in the (1-x)NBT– xCT Raman spectra with increasing CT concentration. In fact, displacement, shifting, and broadening have been observed with x, reflecting chemical modifications at the A-site related to the substitution of Na^+/Bi^{3+} by Ca^{2+}. The results obtained in this study are consistent with those observed as a function of pressure by Kreisel et al. [38] where the same variations and displacements of bands were detected. This proves that the pressure factor and Ca-doped NBT have a similar effect which leads to an important crystalline and vibrational evolution. It is important to note that this observation is applicable only up to $x = 0.55$. For $x \geq 0.65$, the spectra undergo notable variations, where fine and narrow peaks are attributed to

the vibration modes characteristic of pure CT. This confirms that the chemical environment at A-site is modified between x = 0.55 and x = 0.65. This is explained by the probability density of the presence of Ca^{2+} at A-site which increases as a function of x compared to $Na+/Bi^{3+}$ cations, leading to an important amplification of the signal and consequently to an improvement of the characteristic peaks of CT. These modes do not appear for $x \leq 0.55$ due to their low polarizability (CT modes) [39].

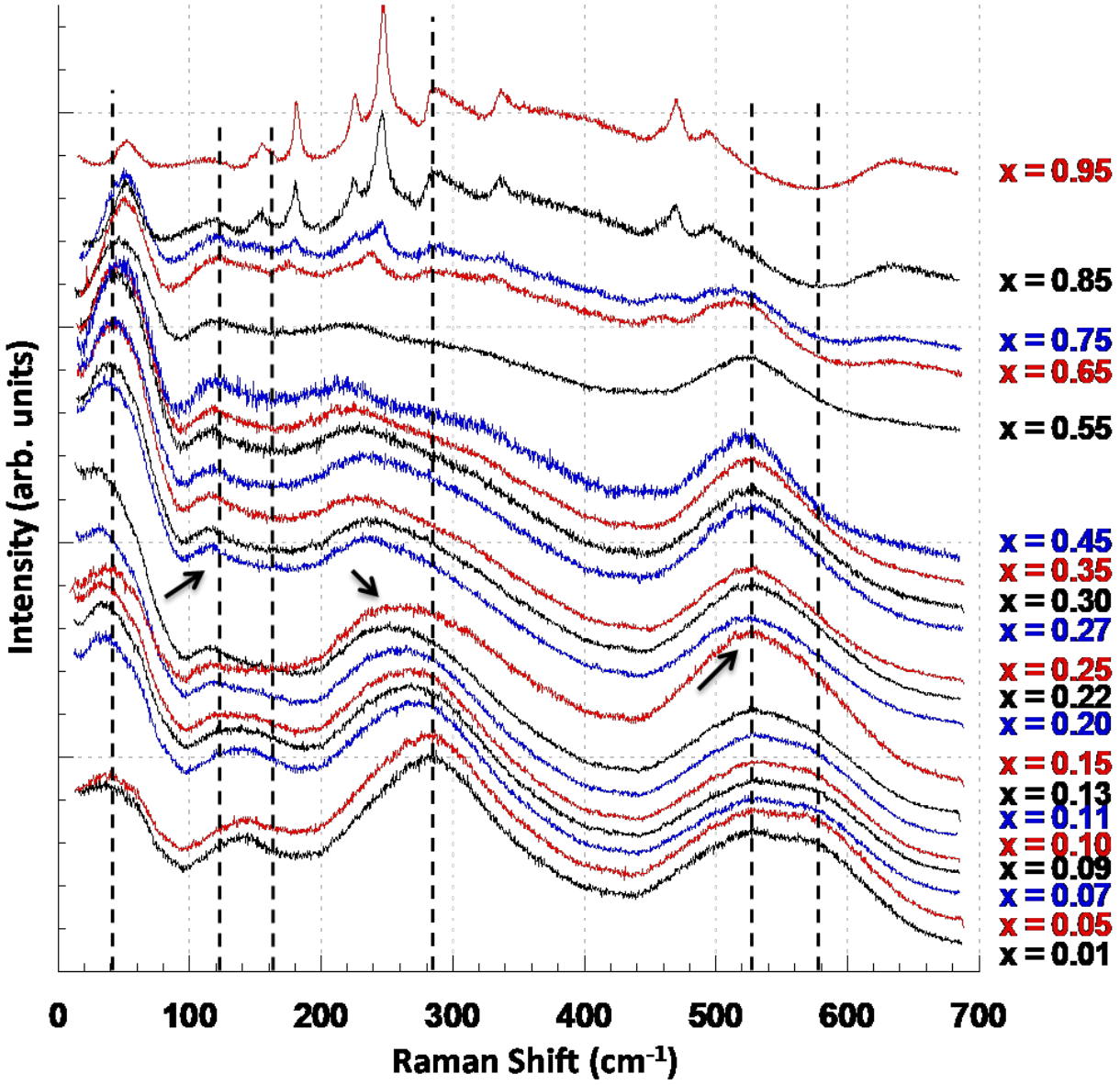

Figure 2: Evolution of Raman spectra for (1-x)NBT – xCT solid solution as a function of x ($0.01 \leq x \leq 0.95$) at room temperature.

In addition, noticeable changes were mainly detected in the high frequency range (over-

lapping modes 400 – 600 cm^{-1}). These modes become increasingly symmetrical and merge into one single mode. During the transition from NBT to CT solid solutions, the ionic radius of A-site decreases ($R_{Na}{}^{+}$ = 1.39 Å, $R_{Bi}{}^{3+}$ = 1.32 Å and $R_{Ca}{}^{2+}$ = 1.34 Å) [40] due to the low substitution observed in NBT. In the work publish by Kreisel et al. [38], the pressure causes a contraction of the crystal lattice of NBT, and consequently, the vibration modes shift to the lower frequencies. Thus, the same phenomenon is obtained with Ca-doped NBT confirming the transition from rhombohedral *(R3c)* phase to orthorhombic *(Pnma)* phase.

Furthermore, the Raman spectra of (1-x)NBT – xCT for $x \leq 0.07$ are very similar to pure NBT retaining the same crystalline structure in this concentration range. However, for high concentration, the bands are shifted to lower frequency, more precisely the two overlapping bands move toward each other ($0.09 \leq x < 0.15$) and merge into a single band for $x \geq 0.15$ reflecting changes in the symmetry in this concentration range. As mentioned previously, the NBT and CT exhibit 13 and 24 Raman-active modes respectively. Therefore, it is reasonable to get differences in the number of modes in Raman spectra for (1-x)NBT – xCT solid solutions with a further increase in x. This reflects the noticeable changes in the Raman spectra obtained for $x \geq 0.65$, contrary to that reported by Birks et al. [28]. For this reason, the Raman spectra of solid solutions are fitted with Lorentzian and Gaussian functions. The obtained fitting parameters (wavenumber (cm^{-1}) and HWHM (cm^{-1})) are plotted as a function of CT concentration in figure 3. HWHM reflects the structural distribution which is inversely proportional to the phonon lifetime. For instance, these two parameters are strong indicator of phase transition in complex perovskite ferroelectrics by their evolution as a function of x or temperature [14]. The identification of phase transition and the structural change are detected by Raman anomalies of HWHM providing information about the changes in the local structure. These anomalies shown as frequency displacement and/or inflexion point at certain composition correspond to phase transitions during which phonons behavior is modified. Similarly, the anomalies detected in the HWHM in our system NBT – CT also reflects the structural change within the material as a function of x and the presence of an MPB. It should be noted that the fit of some spectral profiles (B, C, and D) become difficult when $x > 0.55$ due to the apparition of fine bands characteristics of pure CT. Therefore, the fit is limited to $x = 0.55$.

The variations of the peak frequency and HWHM reveal two successive anomalies at $x = 0.09$ and $x = 0.15$, which appear as discontinuities in the spectral features in regions A to D. These values correspond to the structural changes between the ferroelectric phase *(R3c)* and the relaxor phase *(Pnma)* [33]. Several features can be separately discerned for increasing Ca^{2+} content:

• **Mode A(31 cm^{-1}, Bi–O) :** this band shows that the wavenumber and the corresponding HWHM increase sharply at $x = 0.09$ and become stable up to $x = 0.13$. Then, the wavenumber increases strongly, whereas the HWHM decreases due to the substitution of a high mass ion (Bi^{3+}) by a low mass ion (Ca^{2+}). The values $x = 0.09$ and $x = 0.15$ correspond to the limit composition between the rhombohedral phase *(R3c)* and the orthorhombic phase *(Pnma)* determined by XRD. This variation can't be interpreted as a soft-mode like behavior. This mode is characterized by an abrupt decrease in the frequency toward zero, indicating the disappearance of a band or a change in the position of an atom. In addition,

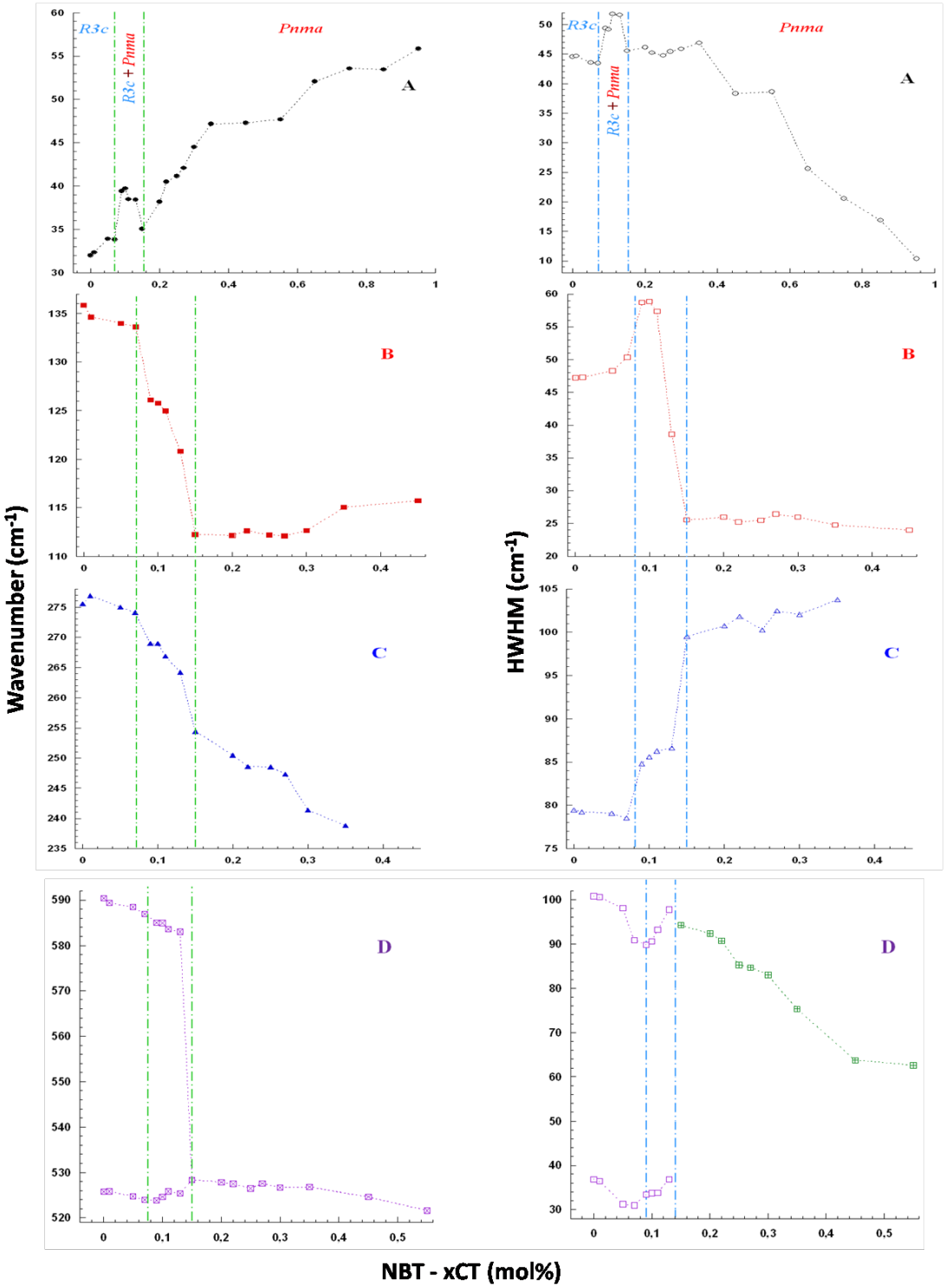

Figure 3: Variation of wavenumber (frequency position) and their corresponding half-width at half maximum (HWHM) of individual bands as a function of x composition for (1-x)NBT – xCT solid solutions at room temperature. Dashed lines are benchmarks to better visualize discontinuities and slope changes associated with phase transitions.

this mode is susceptible to the phase transition since the A-site symmetry is involved. It should be noted that no previous work has discussed the evolution of this peak; its analysis can be carried out from the spectra obtained at different temperatures. It is attributed to a soft-mode of E-symmetry coupled to the F_{2g} mode with close frequency. The increase in CT content is equivalent to a decrease in temperature. This leads to a decrease in the intensity of the central peak, as well as to the splitting of the two vibration modes F_{2g} [31]. For the orthorhombic phase, we notice the disappearance of one of these modes; the band becomes more fine, symmetrical, and shifts towards higher frequency. This modification is associated with Ca-doping that changes the direction of cationic displacement. Only a decrease in the intensity of the central peak is observed [41], while the detailed behavior of these two modes cannot be deduced.

• **Mode B (135 cm^{-1}, Na–O) :** mode B decreases in intensity and shifts towards lower frequencies. It clearly exhibits two anomalies at x = 0.09 and x = 0.15 (Fig. 3-B). It shows a soft-mode behavior up to x = 0.15 and then becomes independent of CT concentration for x $\geq$ 0.20. The HMWM also shows the same changes with x. These changes reveal the transitions occurring in the biphasic domain where the wavenumber and the HWHM for x = 0.13 decrease compared to other compositions (x = 0.09, 0.10, and 0.11). This indicates that the fraction of the orthorhombic phase increases and the material gradually transforms from the rhombohedral *(R3c)* phase to the orthorhombic *(Pnma)* phase. However, for 0.09 $\leq$ x $\leq$ 0.13, the width of the band increases and becomes symmetrical. Then, for x $\geq$ 0.15, the Na–O band undergoes a sudden change becoming narrower and symmetrical. Moreover, for x $\geq$ 0.65, the appearance of new peaks in this frequency range is detected.

• **Mode C (275 cm^{-1} , Ti–O):** the changes produced in this region are related to Ti-cation displacement, which is expected to induce noticeable spectral changes associated with a structural transition. This peak moves linearly for low CT concentration and becomes asymmetric. Then a first anomaly is detected for x = 0.09 where the band shifts towards lower frequency. This displacement is accompanied by a significant increase in width band. A more remarkable second anomaly occurs for x = 0.15. With the sharp decrease of wavenumber and the abrupt increase of HWHM, the mode becomes independent of x for x $\geq$ 0.15, indicating a structural change to the orthorhombic phase. Consequently, the first discontinuity corresponds to the biphasic domain where the rhombohedral *(R3c)* and orthorhombic *(Pnma)* phases coexist. Moreover, the intensity of this band decreases when x increases and finally disappears for x = 0.55. This modification is due to a change of polar feature at B-site associated with the cation displacement towards the center of the octahedron, suggesting a modification of the octahedral tilt ($a^-a^-a^- \rightarrow a^-b^+a^-$). Furthermore, the characteristic modes of CT are observed for x $\geq$ 0.65.

• **Mode D (400 – 600 cm^{-1}):** it consists of broadened two overlapping bands (G and L modes), which are related to the TiO_6 octahedral-distortion. This region is considered sensitive to structural transition based on the hard-mode like behavior [31, 34, 42], and is directly related to the ferroelectric phase transition domain. With increasing CT concentration, band L (Fig.1) moves progressively towards band G (Fig.1), inducing Raman shift (Fig. 3-D). These two bands merge into one band leading to a single mode for x $\geq$ 0.15. This change corresponds to the phase transition from the rhombohedral (*R3c*) phase to

the orthorhombic *(Pnma)* phase. Note that this fusion is nearly similar to the NBT-phase transition induced under pressure by Kreisel et al. [38]. Besides, the intensity of the merged Raman peak becomes weak as CT concentration increases. The fusion of these two bands occurs near the boundary of the rhombohedral – orthorhombic transition. This generates a displacement of the B-cation to the central position of the octahedra in its high symmetry (in agreement with the above discussion for (C) region).

Considering the symmetry of NBT and CT phases, a gradual transition from the rhombohedral structure *(R3c)* to the orthorhombic structure *(Pnma)* is expected when the Ca^{2+} substitution increases. The presence of two anomalies as discontinuities in the Raman spectra (x = 0.09 and x = 0.15) indicates that the transition occurs through an intermediate biphasic domain in which there is a coexistence of two phases *R3c + Pnma*. XRD analysis will confirm these Raman observations.

The results obtained from the Raman spectroscopy and XRD are complementary to each other. Therefore, in light of the present investigations, it can be proved that the MPB of (1-x)NBT – xCT solid solutions lies at the compositions between $0.09 \leq x < 0.15$. The determination of MPB compositions for this system is carried out using different experimental techniques such as dielectric properties [27]. In this work, we found a new limit for MPB not reported previously in the literature. In the work of Ranjan et al. [24, 25], they proved the coexistence of two phases *R3c + Pbnm* for x = 0.10. In addition, we previously reported an unusual thermal hysteresis behavior appearing at x = 0.09 and extending over a concentration range until x = 0.13, identified as MPB [27]. The difference of the exact location of MPB compositions between this study and those reported previously is probably attributed to different synthesis methods and their parameters.

Based on the complementary study by Raman and XRD, the MPB composition is systematically determined. The present results allow identifying the phase boundary between the rhombohedral – orthorhombic phase as the Ca-concentration increases. This new MPB may be used for the development of a new NBT – CT lead-free ceramics system.

3.2. Structural phase transition at room temperature

Figure 4 shows the XRD patterns of the extreme solid solutions (a) NBT (x= 0.00) and (b) CT (x = 1.00) respectively. The obtained diffractograms indicate the presence of a pure crystallized perovskite structure due to the sharp diffraction peaks. These samples are single-phase with no secondary phase, confirming the complete reaction of the formation of NBT and CT solid solutions. The XRD pattern of NBT exhibits peaks characteristic of rhombohedral symmetry with space group *(R3c)* with the presence of superlattice reflexion $(113)_R$ characteristic of this structure. Moreover, the CT diffraction peaks exhibits the characteristic peaks of orthorhombic *(Pnma)* phase. Moreover, the CT structure is identified by the orthorhombic *(Pnma)* vibrational modes in Raman spectroscopy, in contrary to the cubic structure which does not have any Raman active phonon modes for all complex oxide perovskites.

The influence of adding different concentrations of CT was studied. The XRD patterns of (1-x)NBT – xCT solid solutions with $0.01 \leq x \leq 0.95$ are provided in the supplementary material. For all solid solutions, the obtained diffractograms are identical to either pure

NBT or pure CT, depending on the amount of calcium. This system undergoes a phase transition from rhombohedral *(R3c)* to orthorhombic *(Pnma)* with increasing x, confirming the complete formation and the continuity of solid solutions synthesized between NBT and CT systems.

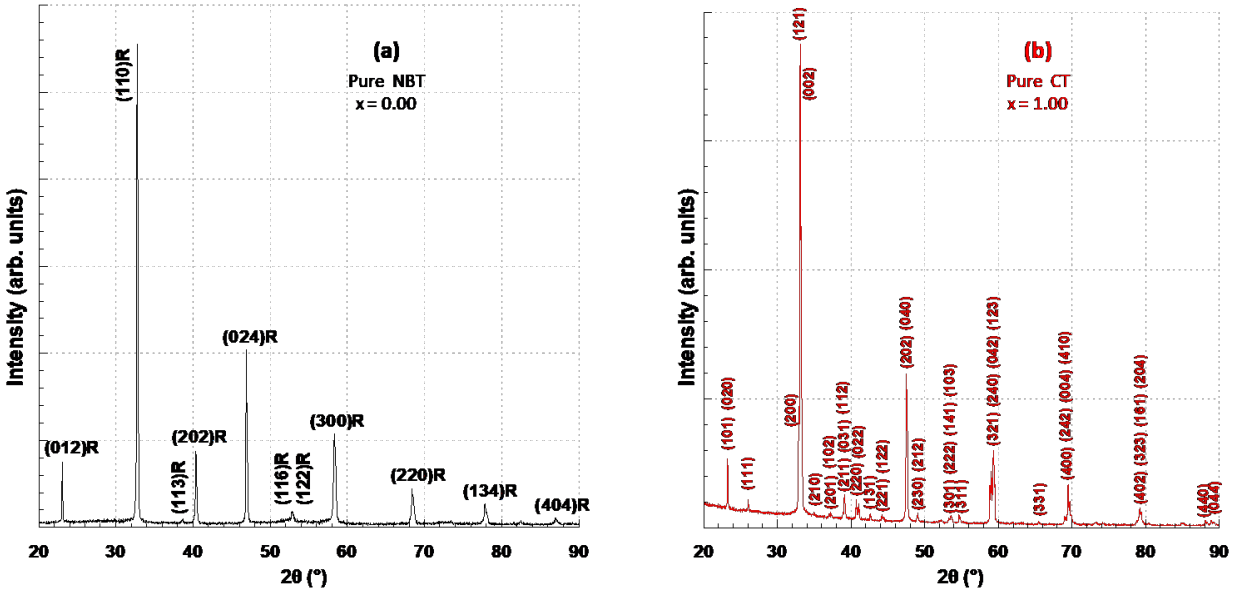

Figure 4: X-ray diffraction patterns of (a) pure NBT (x = 0.00) and (b) pure CT (x = 1.00) solid solutions at room temperature.

Figure 5 displays extended XRD peaks splitting in the 2θ range of 32°-34°, 39°-42° and 67°-72° for various compositions. A gradual shift of the peaks to the higher angle is observed when x increases, indicating a decrease in the lattice parameters. This can be justified by the smaller ionic radius of Ca^{2+} compared to that of Na^{+} and Bi^{3+}. The evolution of the $(104)_R$ $(110)_R$, $(202)_R$, and $(208)_R$ $(220)_R$ rhombohedral peaks revealed that the solid solution undergoes a phase transition from rhombohedral to orthorhombic symmetry. This transition is due to the large distortion caused by increasing CT content at room temperature. Analysis of the evolution of these diffraction peaks as a function of x reveals that:

(i) $\mathbf{x < 0.09}$ **:** the obtained XRD diffraction patterns are identical to that of pure NBT and consequently the structure of these compositions is rhombohedral with *R3c* space group.

(ii) $\mathbf{0.09 \leq x < 0.15}$**:** the XRD patterns show an appearance of additional peaks from x = 0.09, corresponding to $(002)_O$, $(022)_O$, and $(004)_O$ characteristic of the orthorhombic phase. The intensity of these peaks increases with x while the intensity of $(104)_R$ $(110)_R$, $(202)_R$ and $(208)_R$ $(220)_R$gradually decreases until x = 0.13 and then disappears completely for x = 0.15. The $(200)_O$ $(121)_O$ $(002)_O$, $(220)_O$ $(022)_O$, and $(400)_O$ $(242)_O$ $(004)_O$ $(410)_O$ peaks characteristic of the orthorhombic symmetry are also observed. The simultaneous presence of (R + O) peaks in this composition range indicates that both rhombohedral and orthorhombic phases coexist.

(iii) **0.15 ≤ x ≤ 1.00:** an orthorhombic structure with space group *Pnma* was found in this composition range. All the XRD diffraction peaks are identical to those of the orthorhombic *(Pnma)* structure of the pure CT (x = 1.00) phase, with some exception concerning the samples x = 0.45 and 0.55. The diffraction peaks for these two compositions are superimposed and become broader. This is pot*entially due* to a size effect caused by a decrease in crystallite size or to imperfections associated with the creation of micro-distortions and/or stacking-faults (crystallographic defects) [43]. However, it should be noted that these perovskites are occupied by three cations randomly distributed in A-site with a difference in ionic radii (Bi^{3+} = 1.32 Å, Na^{+} = 1.39 Å and Ca^{2+} = 1.34 Å). It is therefore highly probable that the system has a finite size effect of diffracting crystallite which could be responsible for this enlargement. Thus, the structural phase transition from rhombohedral *(R3c)* to orthorhombic *(Pnma)* phase through a mixture of two phases *(R3c + Pnma)* takes place with increasing x at room temperature. These results confirm the formation of NBT–CT solid solutions independently of x.

In our previous study [27], we reported that the system undergoes a phase transition to orthorhombic structure *(Pnma)* where the intensity ratio becomes almost stable for x ≥ 0.15. On the other hand, the drastic increase in the intensity ratio for x > 0.09 is explained by the coexistence of *R3c* phase and *Pnma* phase, corresponding to a reduction of the rhombohedral phase *(R3c)* fraction and to an increase of the orthorhombic phase *(Pnma)* fraction. In addition, we also reported a slight cell volume discontinuity at the limit between the rhombohedral phase and the orthorhombic phase related to the coexistence of two phases *(R3c + Pnma)* at room temperature.

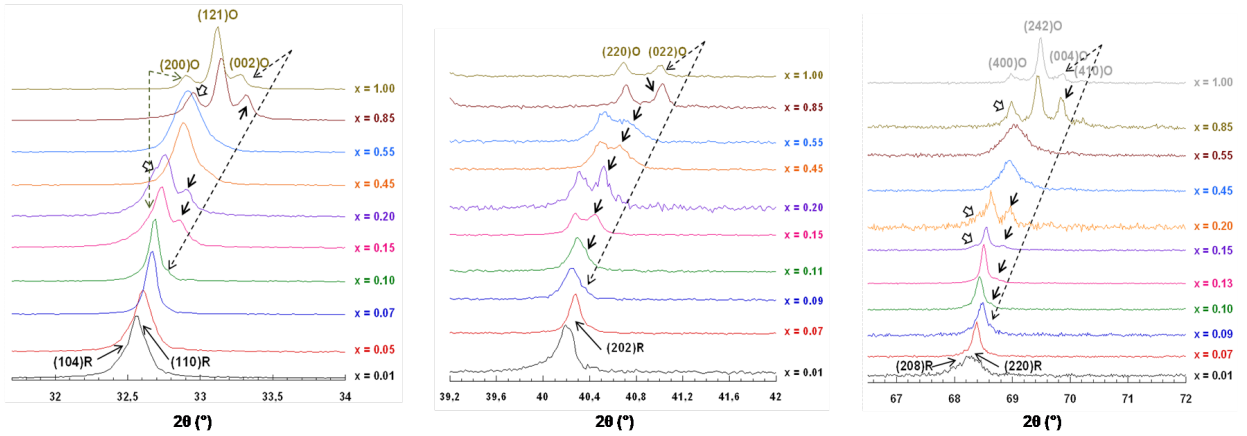

Figure 5: Evolution of XRD peaks of the (1-x)NBT–xCT solid solutions near the MPB region (without the contribution of CuKα_2) in the magnified range 2θ (32°-34°), (39.2°-42°) and (67°-72°). The arrows indicate the appearance of two phases and the structural transition *R3c* to *Pnma* at room temperature. Part of this figure 2θ(67°-72°) has been reproduced from our previous work [27].

A normal biphasic domain and a morphotropic phase boundary (MPB) are constituted by a mixture of two phases with different crystal structures. In the MPB, the biphasic zone consists of identical variable compositions, which means the two phases of similar compositions exist such as NBT–BT rhombohedral and NBT–BT tetragonal for x = 0.07 [9]

and x = 0.55 [44] at room temperature. In addition, the fraction of each phase, the lattice parameters, and the volume change with x. However, in a normal biphasic domain, the two phases have different compositions (x_1 and x_2) while maintaining the same properties independentaly of x. In this work, we have shown that the solid solution is composed of a mixture of two phases in equal compositions and their fractions change with x [27, 42]. Consequently, the obtained results confirm that the mixture of two phases in this region for the (1-x)NBT–xCT system is an MPB.

4. Conclusion

The rhombohedral – orthorhombic morphotropic phase boundary (MPB) in (1-x)NBT – xCT solid solutions was identified by Raman spectroscopy and X-ray diffraction. This system shows a high miscibility of Ca^{2+} at A-site in the entire composition range. A morphotropic phase boundary MPB was confirmed between $0.09 \leq x < 0.15$ by anomalies appearing as discontinuities and distinct changes in room temperature Raman spectra for different solid solutions. The phonon anomalies detected at room temperature for different compositions were discussed in combination with XRD results. The low frequency mode shows a soft-mode like behavior. It shows an anomaly at x = 0.09 and x = 0.15. These values correspond to the limit composition between the rhombohedral *(R3c)* phase and orthorhombic *(Pnma)* phase. Note that the lower frequency mode (31 cm^{-1}) is discussed from the spectra at different temperatures; this mode is original and no previous researches has been discerned it. The high frequency mode displays a hard-mode like behavior showing anomalies at the same composition for x = 0.09 and x = 0.15. This associated with the structural phase transition starts merging into one mode at x = 0.15 and later become symmetrical, which is a clear demonstration of a rhombohedral to orthorhombic phase change passing through by a mixture of two phases. This observation is also verified by thorough X-ray diffraction showing two single phases *(R3c)* and *(Pnma)* separated by an intermediate morphotropic phase boundary (MPB) where the two phases *(R3c + Pnma)* coexist for $0.09 \leq x < 0.15$.

Acknowledgments

This work is supported by the French Ministry of Higher Education and Research, the Nanosciences Department of Université de Bourgogne Franche-Comté (UBFC), and the Lebanese American University.

References

[1] G. H. Haertling, Ferroelectric Ceramics: History and Technology, Journal of the American Ceramic Society 82 (4) (1999) 797–818.

[2] W. Jo, J. E. Daniels, J. L. Jones, X. Tan, P. A. Thomas, D. Damjanovic, J. Rödel, Evolving morphotropic phase boundary in lead-free (Bi1/2Na1/2)TiO3-BaTiO3 piezoceramics, Journal of Applied Physics 109 (2011) 14110–014117.

[3] B. Jaffe, W. R. Cook, H. Jaffe, Piezoelectric Ceramics. Academic London (1971).

[4] A. Ibrahim, R. Murgan, M. K. A. Rahman, J. Osman, Morphotropic phase boundary in ferroelectric materials, in: M. Lallart (Ed.), Ferroelectrics: Physical Effects, BoD, 2011.

[5] H. Fu, R. E. Cohen, Polarization rotation mechanism for ultrahigh electromechanical response in single-crystal piezoelectrics, Nature 403 (6767) (2000) 281–283.
[6] J. Rödel, W. Jo, K. T. P. Seifert, E.-M. Anton, T. Granzow, D. Damjanovic, Perspective on the Development of Lead-free Piezoceramics, Journal of the American Ceramic Society 92 (6) (2009) 1153–1177.
[7] T. Tadashi, M. Kei-Ichi, S. Koichiro, Bi1/2Na1/2)TiO3-BaTiO3 System for Lead-Free Piezoelectric Ceramics, Japanese Journal of Applied Physics 30 (1991) 2236–2236.
[8] B.-J. Chu, D.-R. Chen, G.-R. Li, Q.-R. Yin, Electrical properties of Na1/2Bi1/2TiO3-BaTiO3 ceramics, Journal of the European Ceramic Society 22 (2002) 2115–2121.
[9] M. Chen, Q. Xu, B. H. Kim, Structure and electrical properties of (Na0.5Bi0.5)1−xBaxTiO3 piezoelectric ceramics, Journal of the European Ceramic Society 28 (2008) 843–849.
[10] Y. Li, W. Chen, J. Zhou, Dielectric and ferroelectric properties of lead-free Na0.5Bi0.5TiO3-K0.5Bi0.5TiO3 ferroelectric ceramics, Ceramics International 31 (2005) 139–142.
[11] H. Xie, L. Jin, D. Shen, X. Wang, G. Shen, Morphotropic phase boundary, segregation effect and crystal growth in the NBT–KBT system, Journal of Crystal Growth 311 (14) (2009) 3626–3630.
[12] M. Otoničar, S. D. Škapin, M. Spreitzer, D. Suvorov, Compositional range and electrical properties of the morphotropic phase boundary in the Na0.5Bi0.5TiO3–K0.5Bi0.5TiO3 system, Journal of the European Ceramic Society 30 (4) (2010) 971–979. doi:10.1016/j.jeurceramsoc.2009.10.006.
[13] J. R. Gomah-Pettry, P. Marchet, A. Salak, V. M. Ferreira, J. P. Mercurio, Electrical Properties of Na0.5Bi0.5TiO3 – SrTiO3 Ceramics, Integrated Ferroelectrics 61 (1) (2004) 159–162.
[14] D. Rout, K. S. Moon, S.-J. L. Kang, Dielectric and Raman scattering studies of phase transitions in the (100 - x)Na0.5Bi0.5TiO3–xSrTiO3 system, Journal of Applied Physics 108 (2010) 84102–084107.
[15] W. Krauss, D. S. tz, F. A. Mautner, Piezoelectric properties and phase transition temperatures of the solid solution of (1 - x)(Bi0.5Na0.5)TiO3-xSrTiO3, Journal of the European Ceramic Society 30 (2010) 1827–1832.
[16] G. O. Jones, P. A. Thomas, The tetragonal phase of Na0.5Bi0.5TiO3– a new variant of the perovskite structure, Acta Crystallographica Section B Structural Science 56 (3) (2000) 426–430.
[17] G. O. Jones, P. A. Thomas, Investigation of the structure and phase transitions in the novel A-site substituted distorted perovskite compound Na0.5Bi0.5TiO3, Acta Crystallographica Section B Structural Science 58 (2) (2002) 168–178.
[18] V. Dorcet, G. Trolliard, P. Boullay, Reinvestigation of Phase Transitions in Na0.5Bi0.5TiO3by TEM. Part I: First Order Rhombohedral to Orthorhombic Phase Transition, Chemistry of Materials 20 (15) (2008) 5061–5073.
[19] S. E. Park, K. S. Hong, Variations of Structure and Dielectric Properties on Substituting A-site Cations for Sr2+ in (Na1/2Bi1/2)TiO3, Journal of Materials Research 12 (1997) 2152–2157.
[20] J. Gomah-Pettry, Sodium-bismuth titanate based lead-free ferroelectric materials, Journal of the European Ceramic Society 24 (6) (2004) 1165–1169.
[21] J. R. Gomah-Pettry, A. N. Salak, P. Marchet, V. M. Ferreira, J. P. Mercurio, Ferroelectric relaxor behaviour of Na0.5Bi0.5TiO3–SrTiO3 ceramics (2004). doi:10.1002/pssb.200302020.
[22] Y. Hiruma, Y. Imai, Y. Watanabe, Large electrostrain near the phase transition temperature of (Bi0.5Na0.5)TiO3–SrTiO3 ferroelectric ceramics, Applied Physics Letters 92 (2008) 262904–262903.
[23] V. Dorcet, G. Trolliard, P. Boullay, The structural origin of the antiferroelectric properties and relaxor behavior of Na0.5Bi0.5TiO3, Journal of Magnetism and Magnetic Materials 321 (11) (2009) 1758–1761.
[24] R. Ranjan, V. Kothai, R. Garg, A. Agrawal, A. Senyshyn, H. Boysen, Degenerate rhombohedral and orthorhombic states in Ca-substituted Na0.5Bi0.5TiO3, Applied Physics Letters 95 (4) (2009) 042904–042904.
[25] R. Ranjan, R. Garg, V. Kothai, A. Agrawal, A. Senyshyn, H. Boysen, Phases in the (1 −x)Na0.5Bi0.5TiO3–(x)CaTiO3system, Journal of Physics: Condensed Matter 22 (7) (2010) 075901–075901.
[26] H. L. Du, X. Du, H. L. Li, Phase structure and electrical properties of lead free Na0·5Bi0·5TiO3–CaTiO3ceramics, Advances in Applied Ceramics 112 (5) (2013) 277–281.

[27] R. Roukos, S. A. Dargham, J. Romanos, F. Barakat, D. Chaumont, Complex structural contribution of the morphotropic phase boundary in Na0.5Bi0.5TiO3 - CaTiO3 system, Ceramics International 45 (4) (2019) 4467–4473. doi:10.1016/j.ceramint.2018.11.126.

[28] E. Birks, M. Dunce, R. Ignatans, A. Kuzmin, A. Plaude, M. Antonova, K. Kundzins, A. Sternberg, Structure and dielectric properties of Na0.5Bi0.5TiO3-CaTiO3 solid solutions, Journal of Applied Physics 119 (7) (2016) 074102–074102.

[29] R. Roukos, J. Romanos, S. A. Dargham, D. Chaumont, Quantification of relaxor behavior in (1 − x)Na0.5Bi0.5TiO3 – xCaTiO3 lead-free ceramics system, Journal of the European Ceramic Society 39 (7) (2019) 2297–2303.

[30] J. Kreisel, P. Bouvier, B. Dkhil, P. A. Thomas, A. M. Glazer, T. R. Welberry, B. Chaabane, M. Mezouar, High-pressure x-ray scattering of oxides with a nanoscale local structure: Application toNa1/2Bi1/2TiO3, Physical Review B 68 (1) (2003) 14113–14113.

[31] J. Petzelt, S. Kamba, J. F. bry, Raman and high-frequency dielectric spectroscopy and the phase transitions in Na1/2Bi1/2TiO3, Journal of Physics: Condensed Matter 16 (2004) 2719–2719.

[32] L. Luo, W. Ge, J. Li, Raman spectroscopic study of Na1/2Bi1/2TiO3-x%BaTiO3 single crystals as a function of temperature and composition, Journal of Applied Physics 109 (2011) 113507–113506.

[33] R. Roukos, N. Zaiter, D. Chaumont, Relaxor behaviour and phase transition of perovskite ferroelectrics-type complex oxides (1–x)Na0.5Bi0.5TiO3–xCaTiO3 system, Journal of Advanced Ceramics 7 (2) (2018) 124–142.

[34] J. Kreisel, A. M. Glazer, P. Bouvier, G. Lucazeau, High-pressure Raman study of a relaxor ferroelectric: TheNa0.5Bi0.5TiO3 perovskite, Physical Review B 63 (17) (2001) 174106–174106.

[35] B. K. Barick, K. K. Mishra, A. K. Arora, R. N. P. Choudhary, D. K. Pradhan, Impedance and Raman spectroscopic studies of (Na0.5Bi0.5)TiO3, Journal of Physics D: Applied Physics 44 (35) (2011) 355402–355402.

[36] H. Zheng, G. C. de Györgyfalva, R. Quimby, H. Bagshaw, R. Ubic, I. M. Reaney, J. Yarwood, Raman spectroscopy of B-site order–disorder in CaTiO3-based microwave ceramics, Journal of the European Ceramic Society 23 (14) (2003) 2653–2659.

[37] M. Guennou, P. Bouvier, B. Krikler, J. Kreisel, R. Haumont, G. Garbarino, High-pressure investigation ofCaTiO3up to 60 GPa using x-ray diffraction and Raman spectroscopy, Physical Review B 82 (13) (2010) 134101–134101.

[38] J. Kreisel, P. Bouvier, High-pressure Raman spectroscopy of nano-structured ABO3 perovskites: a case study of relaxor ferroelectrics, Journal of Raman Spectroscopy 34 (7-8) (2003) 524–531.

[39] T. Hirata, K. Ishioka, M. Kitajima, Vibrational Spectroscopy and X-Ray Diffraction of Perovskite Compounds Sr1−xMxTiO3(M= Ca, Mg; 0 ≤x≤ 1), Journal of Solid State Chemistry 124 (2) (1996) 353–359.

[40] Y. Yuan, C. J. Zhao, X. H. Zhou, B. Tang, S. R. Zhang, High-temperature stable dielectrics in Mn-modified (1-x) Bi0.5Na0.5TiO3-xCaTiO3 ceramics, Journal of Electroceramics 25 (2-4) (2010) 212–217.

[41] I. G. Siny, E. Husson, J. M. Beny, S. G. Lushnikov, E. A. Rogacheva, P. P. Syrnikov, A central peak in light scattering from the relaxor-type ferroelectric Na1/2Bi1/2TiO3, Physica B: Condensed Matter 293 (3-4) (2001) 382–389.

[42] J. Kreisel, A. M. Glazer, G. Jones, P. A. Thomas, L. Abello, G. Lucazeau, An x-ray diffraction and Raman spectroscopy investigation of A-site substituted perovskite compounds: the (Na1-xKx)0.5Bi0.5TiO3(0lexle1) solid solution, Journal of Physics: Condensed Matter 12 (14) (2000) 3267–3280.

[43] K. Datta, K. Roleder, P. A. Thomas, Enhanced tetragonality in lead-free piezoelectric (1−x)BaTiO3–xNa1/2Bi1/2TiO3 solid solutions where x=0.05–0.40, Journal of Applied Physics 106 (12) (2009) 123512–123512.

[44] D. Rout, K. S. Moon, V. S. Rao, Study of the morphotropic phase boundary in the lead-free Na1/2Bi1/2TiO3-BaTiO3 system by Raman spectroscopy, Journal of the Ceramic Society of Japan 117 (2009) 797–800.